Supporting Information

Donnelly et al. 10.1073/pnas.1708838115

SI Experimental Procedures

Animals. All experiments were carried out in compliance with the guidelines of the Association for Assessment and Accreditation of Laboratory Animal Care International and approved by the Institutional Animal Care and Use Committee of the University of Michigan.

Fixation, Sectioning, and Immunostaining. GGs and TGs were collected and fixed overnight in 4% paraformaldehyde at 4 °C, while tongues were dissected within the mandible and fixed for 2 to 3 h, dissected free from the mandible, and fixed for another 2 to 3 h at room temperature. Tissues were cryopreserved, embedded in OCT (Tissue-Tek; VWR), and stored at −80 °C until sectioning. GGs and TGs were sectioned at a thickness of 20 μm on a cryostat (CM1950; Leica Biosystems), except for one cohort of animals, where sections were produced at 40 μm. In all cases, sections were collected serially. Tongues were sectioned at a thickness of 20 μm for Ret and GDNF expression tracing experiments, while 50-μm sections were produced and collected serially for the analysis of Ret knockout mice to avoid double counting FPs. For immunostaining, sections were first rehydrated in PBS for 30 min at room temperature, following by blocking in 10% normal donkey serum (Jackson ImmunoResearch), 0.25 to 0.5% BSA (Sigma), and mouse-on-mouse blocking reagent (1 drop per 1.5 mL blocking solution; Vector Laboratories) in 0.3% Triton X-100/PBS (PBS-X). Following blocking, the following primary antibodies were diluted in 0.3% PBS-X and incubated on the sections overnight at 4 °C (48 h at 4 °C for 50-μm tongue sections) in a humidified chamber: α-RFP (1:200 to 1:500; 600-401-379; Rockland), α-Phox2b (1:200 to 1:500; AF4940; R&D), α-TuJ1 (βIII-tubulin; 1:200; T8578; Sigma), α-TrkB (1:250 to 1:400; AF1494; R&D), α-Brn3a/Pou4f1 (1:25; MAB1585; Millipore), α-P2X3 (1:200 to 1:400; AB5895; Millipore), α-GFRα1 (1:50; AF560; R&D), α-GFRα2 (1:100; AF429; R&D), α-GFRα3 (1:100; AF2645; R&D), α-NF200 (1:200 to 1:500; NFH; Aves Labs; combined with 1:500; ab8135; Abcam), α-Islet1 [1:200; 39-4D5-s; Developmental Studies Hybridoma Bank (DSHB)], α–cytokeratin-8 [TROMA-I; 1:50 (supernatant); DSHB], and α–E-cadherin (1:1,000 to 1:2,000; AF748; R&D). Slides were washed three or four times with 0.3% PBS-X, and secondary antibodies against the intended species were added at a concentration of 1:200 (GGs and TGs) or 1:400 (tongues) (all raised in donkey; CF488, CF543, or CF633; Biotium). After secondary antibody incubation, slides were washed with 0.3% PBS-X three times, followed by washes in PBS. Slides were coverslipped with DAPI Fluoromount-G (Southern Biotech) and stored in darkness until imaging. All imaging was performed on a Leica SP5 confocal microscope using LAS-AF software (Leica Microsystems). Images were taken at 20× or 63× magnification with high resolution (2,048 × 2,048) and a *z*-step size of 1 μm (tongues) or 2.0 μm (GGs and TGs). For tongues, every FP (identified using DAPI) was imaged in its entirety (15 to 25 optical sections). For GGs and TGs, every section containing neurons (identified using the TuJ1 channel) was imaged. Maximum projection and median noise reduction (pixel width of 5 kernels; LAS software; Leica Biosystems) was applied to all files to generate a single composite image for all subsequent analyses.

Fiji Quantification of Fungiform Papilla Innervation and Phox2b Expression. All FPs from 50-μm sections produced from E18.5 $Ret^{+/+}$ and $Ret^{-/-}$ anterior tongues were imaged in their entirety. During both image capture and analysis, the experimenters were naïve to the experimental conditions. All imaging of individual papillae took place at 63× magnification. Following image collection and processing, images were imported into ImageJ using the Fiji image-processing package (45). Quantifications were performed in two ways: quantification of the P2X3+ and TuJ1+ pixels within the K8+ region, or quantification of the K8+, P2X3+, and TuJ1+ pixels within the entire fungiform papilla. The K8+ region was defined by setting the threshold to 1 and outlining all positive pixels, while the basal epithelium defining the fungiform papilla trench was used to delineate the entire fungiform papilla. Once the borders surrounding the full fungiform papilla or K8+ region were determined, the channels were split and converted to grayscale, and thresholds were set for each channel to minimize inclusion of background quantification. To control for variability in the threshold setting, all quantifications were performed by two independent investigators (naïve to experimental conditions) and averaged together. Quantifications with greater than 10% variability were omitted. For the experiments analyzing residual Phox2b expression in Ret germ-line knockout mice, GGs were collected, sectioned, and imaged as described above. Channels were separated and converted to grayscale, and individual neurons were sampled by an observer naïve to experimental conditions. The data are reported as the mean pixel count per GG neuron ± SEM.

Tissue Lysis and Quantitative Immunoblotting. Spinal cords were harvested from 1NM-PP1–treated $Ret^{fx/+}$ and $Ret^{fx/-}$ mice at E18.5 (Fig. 3), and GGs from P0 and adult C57BL/6J mice (strain 000664; Jackson Laboratory) were placed in a 2.0-mL tube with 250 μL lysis buffer (pH 7.4 Tris-buffered saline, 10% glycerol, 500 μM sodium vanadate, and complete protease inhibitors) lacking detergent, along with a steel grinding ball (5 mm; Qiagen). For the experiments utilizing GGs, ganglia were collected bilaterally along with the facial nerve, and three animals were pooled for each tube to increase protein yields. Tissues were then mechanically homogenized using the TissueLyser II (Qiagen) at a frequency of 20 Hz for 5 min. The homogenates were mixed with equal volumes of lysis buffer containing 2% Nonidet P-40 and incubated for 1 h at 4 °C under gentle agitation. Homogenates were then centrifuged for 10 min at 16,100 × *g* twice to remove insoluble material. Samples were then prepared for SDS-polyacrylate gel electrophoresis (SDS/PAGE) by adding 2× sample buffer (pH 6.8 Tris-buffered saline, 20% glycerol, 10% β-mercaptoethanol, 0.05% bromophenol blue, and 4% SDS) and boiling the samples. Samples for Western blotting were subjected to SDS/PAGE followed by electroblotting onto polyvinylidene difluoride membranes (Immobilon-P; Millipore). Western blot analysis was performed using the following antibodies at the indicated concentrations: α-Ret (AF482; 1:1,000; R&D) and α-actin (JLA-20; 1:2,000; Iowa Hybridoma). For quantifications, scanned images of X-ray films were imported into ImageJ (NIH) and processed using the gel analysis toolkit. Integrated density values were reported as the mean ± SEM in arbitrary units on the vertical axis. Total Ret levels were normalized to actin as a loading control. 1NM-PP1 experiments were performed on $n = 7$ $Ret^{fx/+}$ and $n = 10$ $Ret^{fx/-}$ mice from three separate litters. Experiments comparing P0 vs. adult expression of Ret in the GG were performed on five (P0) or six (adult) separate lysates.

Verification of Diphtheria Toxin Ablation. Ret+ neuron ablation was verified in TMX-treated *Ret*-Cre/ER^{T2}; $Rosa26^{LSL\text{-}DTA/LSL\text{-}DTA}$

mice by serially sectioning GGs of $Ret^{+/+}$; $DTA^{+/+}$ and $Ret^{Cre/+}$; $DTA^{+/+}$ mice and performing Phox2b counts. Ret-ablated mice having full electrophysiological traces and demonstrating a loss of Phox2b+ neurons greater than one statistical deviation from the mean of the control group (a number chosen based on the adult expression data) were subsequently included in the analysis, while those not meeting these criteria were excluded.

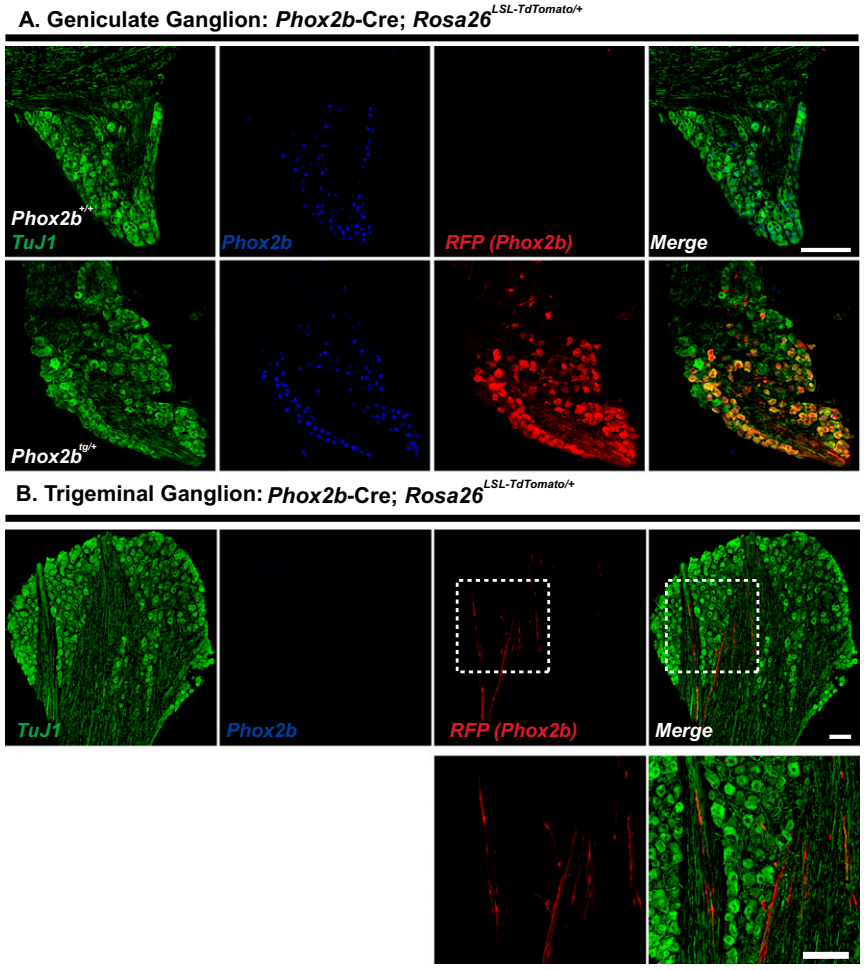

Fig. S1. Characterization of *Phox2b*-Cre$^{tg/+}$ mice and Phox2b immunostaining. (*A*) GGs were collected from P0 *Phox2b*-Cre$^{+/+}$; *Rosa26*$^{LSL\text{-}TdTomato/+}$ (*Upper*) or *Phox2b*-Cre$^{tg/+}$; *Rosa26*$^{LSL\text{-}TdTomato/+}$ (*Lower*) and stained for TuJ1 (green), Phox2b (blue), and RFP (indicates Ret; red), with the merged image displayed (*Right*). Nearly complete overlap (98.84 ± 0.11%) was observed of Phox2b immunoreactivity and RFP staining, indicating high reliability of Phox2b immunostaining. (*B*) TGs from *Phox2b*-Cre$^{tg/+}$; *Rosa26*$^{LSL\text{-}TdTomato/+}$ mice had a nearly complete absence of Phox2b immunoreactivity (blue) and a corresponding absence of RFP labeling, further validating Phox2b immunostaining and the *Phox2b*-Cre$^{tg/+}$ reporter. Areas within dash boxes are magnified (*Bottom*). Similar results were observed in GGs from $n = 4$ separate mice. (Scale bars, 100 μm.)

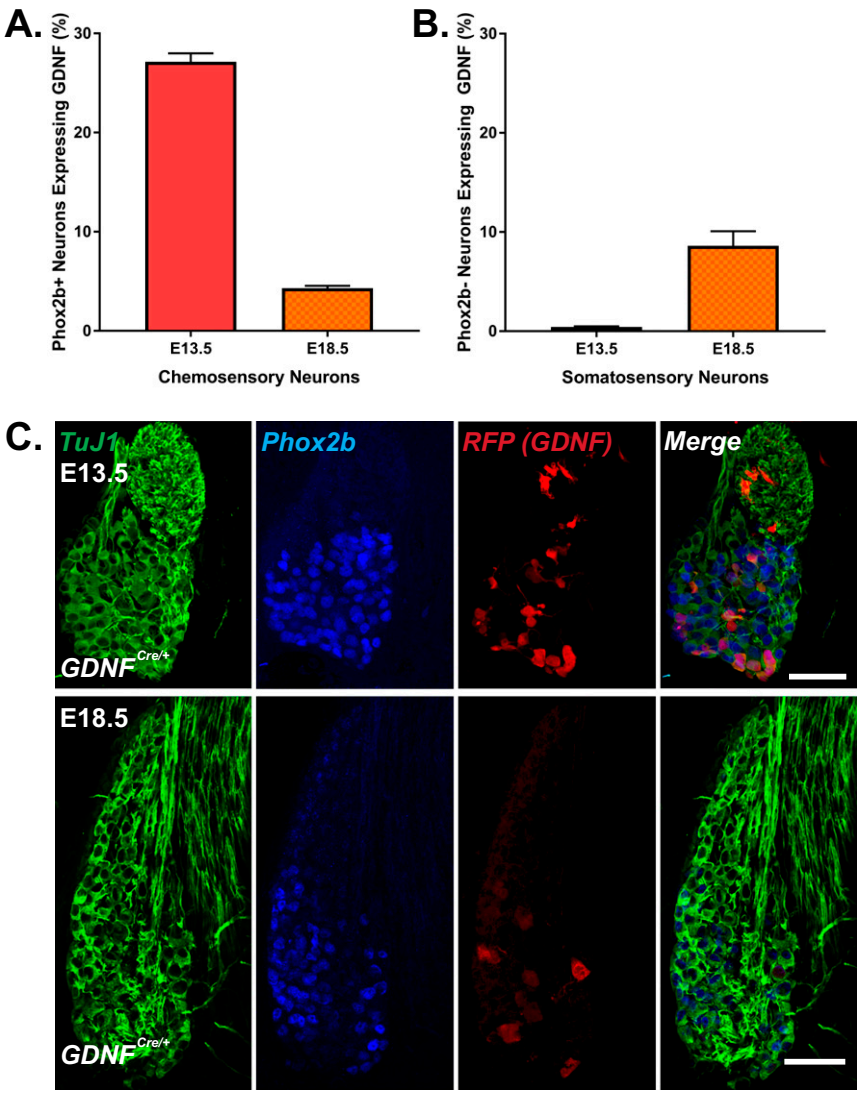

Fig. S2. GDNF is expressed by chemosensory geniculate ganglion neurons early in development. Tamoxifen (TMX) was administered to *GDNF*-IRES-Cre/ER^{T2}; *Rosa26*$^{LSL\text{-}TdTomato/+}$ reporter mice at E9.5 to E12.5 with E13.5 analysis and E14.5 to E17.5 with E18.5 analysis. (*A*) Quantification of GDNF expression indicates that many chemosensory neurons express GDNF at E13.5 but expression is largely absent by E18.5 (n = 3 at each age). (*B*) Few somatosensory geniculate neurons express GDNF at either time point. (*C*) Immunostaining of E13.5 and E18.5 geniculate ganglia taken from *GDNF*-IRES-Cre/ER^{T2}; *Rosa26*$^{LSL\text{-}TdTomato/+}$ reporter mice, stained with TuJ1 (green), Phox2b (blue), and RFP (indicating Ret; red), with merged images (*Right*). Error bars indicate mean ± SEM. (Scale bars, 100 μM.)

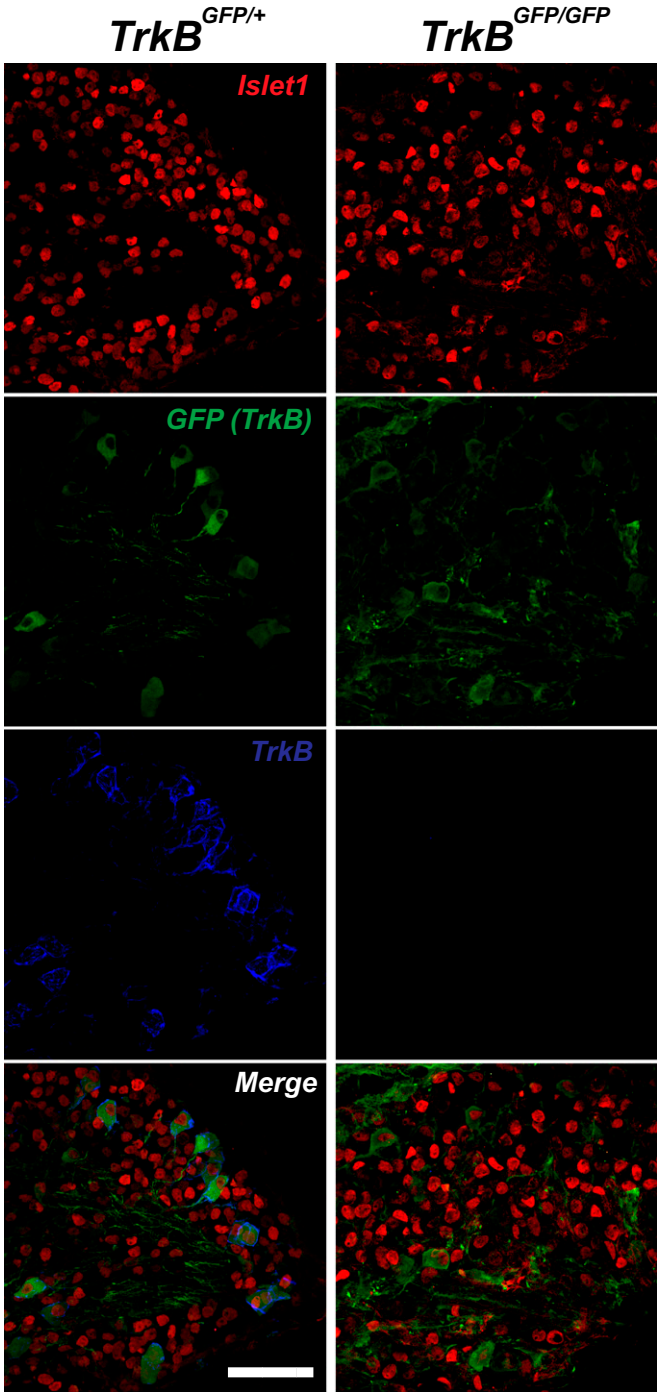

Fig. S3. Validation of TrkB immunostaining. Heads from P0 heterozygous $TrkB^{GFP/+}$ (one functional copy of TrkB protein; *Left*) or homozygous $TrkB^{GFP/GFP}$ (no TrkB protein produced; *Right*) mice were sectioned and immunostained for Islet1 (pan sensory marker; red), GFP (indicating cells normally expressing TrkB; green), and TrkB (labeling actual TrkB protein; blue). Trigeminal ganglia were imaged. Nearly complete overlap of GFP and TrkB staining was observed in $TrkB^{GFP/+}$ neurons, while no TrkB staining was observed in $TrkB^{GFP/GFP}$ ganglia, despite the remaining presence of TrkB+ large-diameter neurons. These data provide evidence for reliable TrkB immunostaining using this antibody and immunostaining method. Similar results were observed from $n = 3$ separate TGs. (Scale bar, 50 μm.)

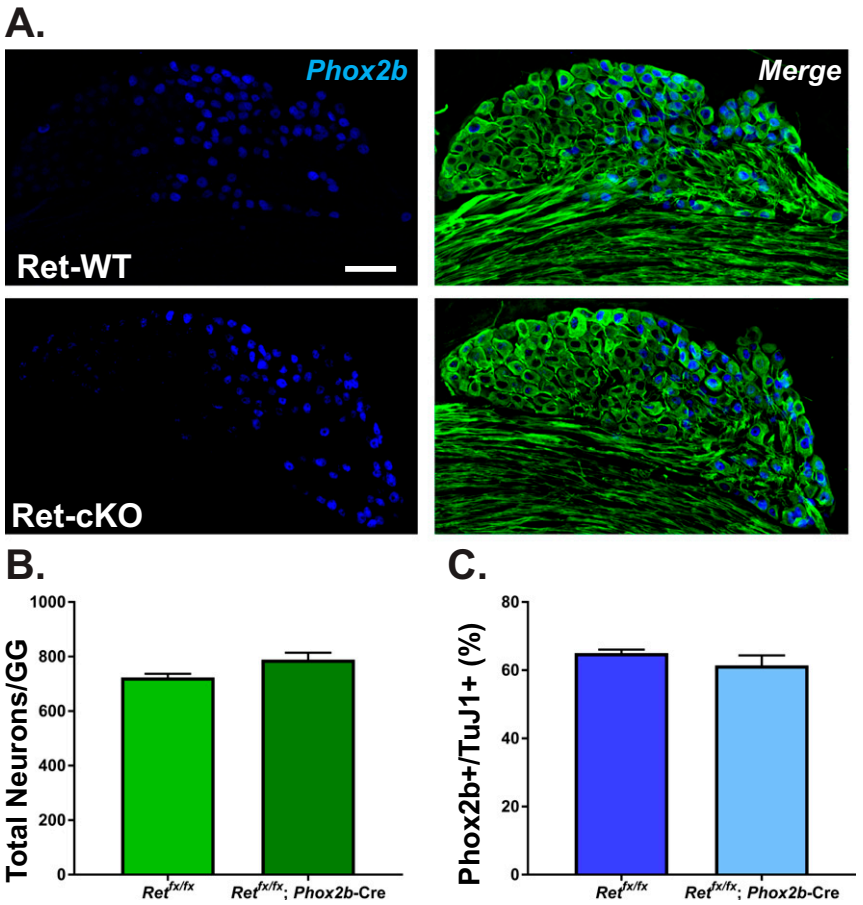

Fig. S4. Ret is dispensable for the maintenance of Phox2b. (*A*) *Ret*$^{fx/fx}$ and *Ret*$^{fx/fx}$; *Phox2b*-Cre$^{tg/+}$ GGs were immunostained for TuJ1 (green) and Phox2b (blue). No qualitative differences were observable in size of the GG or in Phox2b immunoreactivity. (*B*) Quantification of total neuron numbers found no significant differences between *Ret*$^{fx/fx}$ ($n = 5$) and *Ret*$^{fx/fx}$; *Phox2b*-Cre$^{tg/+}$ ($n = 7$) GGs ($P = 0.0712$). (*C*) No difference was observed in the proportion of neurons expressing Phox2b ($n = 5$ to 7; $P = 0.3403$). Error bars indicate mean ± SEM. (Scale bar, 100 μm.)

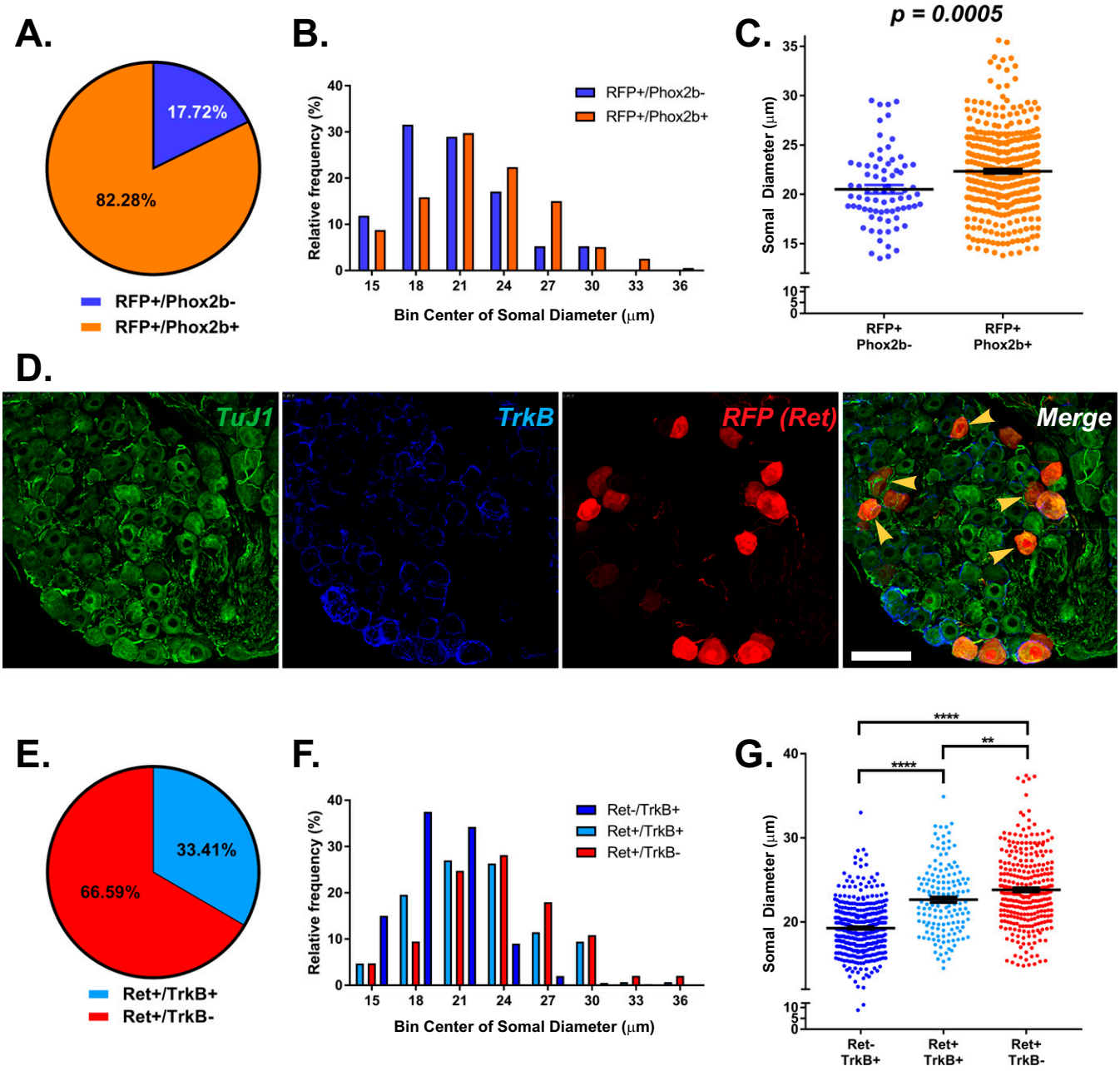

Fig. S5. Characterization of Ret+ adult geniculate ganglion neurons. (*A*) Classification of Phox2b expression in *Ret*-Cre/ER^{T2}; *Rosa26*$^{LSL\text{-}TdTomato/+}$ reporter mice given TMX as described in Fig. 5; 82.28% of all Ret+ neurons counted from $n = 5$ mice were chemosensory (Phox2b+). (*B*) Histogram displaying the distribution of somal diameters, measured at the widest aspect of each RFP+ (Ret-expressing) neuron, in RFP+ chemosensory (Phox2b+) and somatosensory (Phox2b−) GG neurons. A trend was observed for RFP+/Phox2b+ neurons to be larger in diameter compared with RFP+/Phox2b− neurons ($P = 0.0005$). (*C*) Graphical representation of the somal diameter of RFP+/Phox2b− (blue dots) and RFP+/Phox2b+ neurons (orange dots), with the mean somal diameters indicated by the black lines. Many more chemosensory Ret+ neurons were >30 μm in somal diameter. Two-tailed *t* test indicated that the RFP+/Phox2b+ neurons were significantly larger than RFP+/Phox2b− neurons ($P = 0.0005$). (*D*) Characterization of overlap in Ret expression with TrkB protein expression in *Ret*-Cre/ER^{T2}; *Rosa26*$^{LSL\text{-}TdTomato/+}$ reporter GGs administered TMX as described in Fig. 5. Ret expression was observed to be more restricted compared with TrkB. Examples of RFP+/TrkB+ and RFP+/TrkB− (yellow arrowheads) neurons could be observed. (*E*) Classification of overlap in RFP and TrkB expression ($n = 4$). Approximately two-thirds of neurons expressed Ret but not TrkB, while one-third of neurons expressed both receptors. (*F*) Histogram displaying the distribution of somal diameters in Ret−/TrkB+ (dark blue bars), Ret+/TrkB+ (light blue bars), and Ret+/TrkB− (red bars) GG neurons. As in *B*, the somal diameter of Ret+/TrkB− neurons was shifted to the right (larger) compared with Ret+/TrkB+ and Ret−/TrkB+ neurons. (*G*) Graphical representation of the somal diameter of Ret−/TrkB+ (dark blue dots), Ret+/TrkB+ (light blue dots), and Ret+/TrkB− (red dots), with the mean indicated by the black bars. A statistically significant increase in somal diameter was observed (one-way ANOVA) between all groups, with Ret+/TrkB− being significantly larger than Ret+/TrkB+ ($P = 0.0058$) and Ret−/TrkB+ ($P < 0.0001$) neurons. Ret+/TrkB+ neurons were also found to be significantly larger than Ret−/TrkB+ neurons ($P < 0.0001$). Error bars indicate mean ± SEM; $^{**}P < 0.01$, $^{****}P < 0.0001$. (Scale bar, 50 μm.)

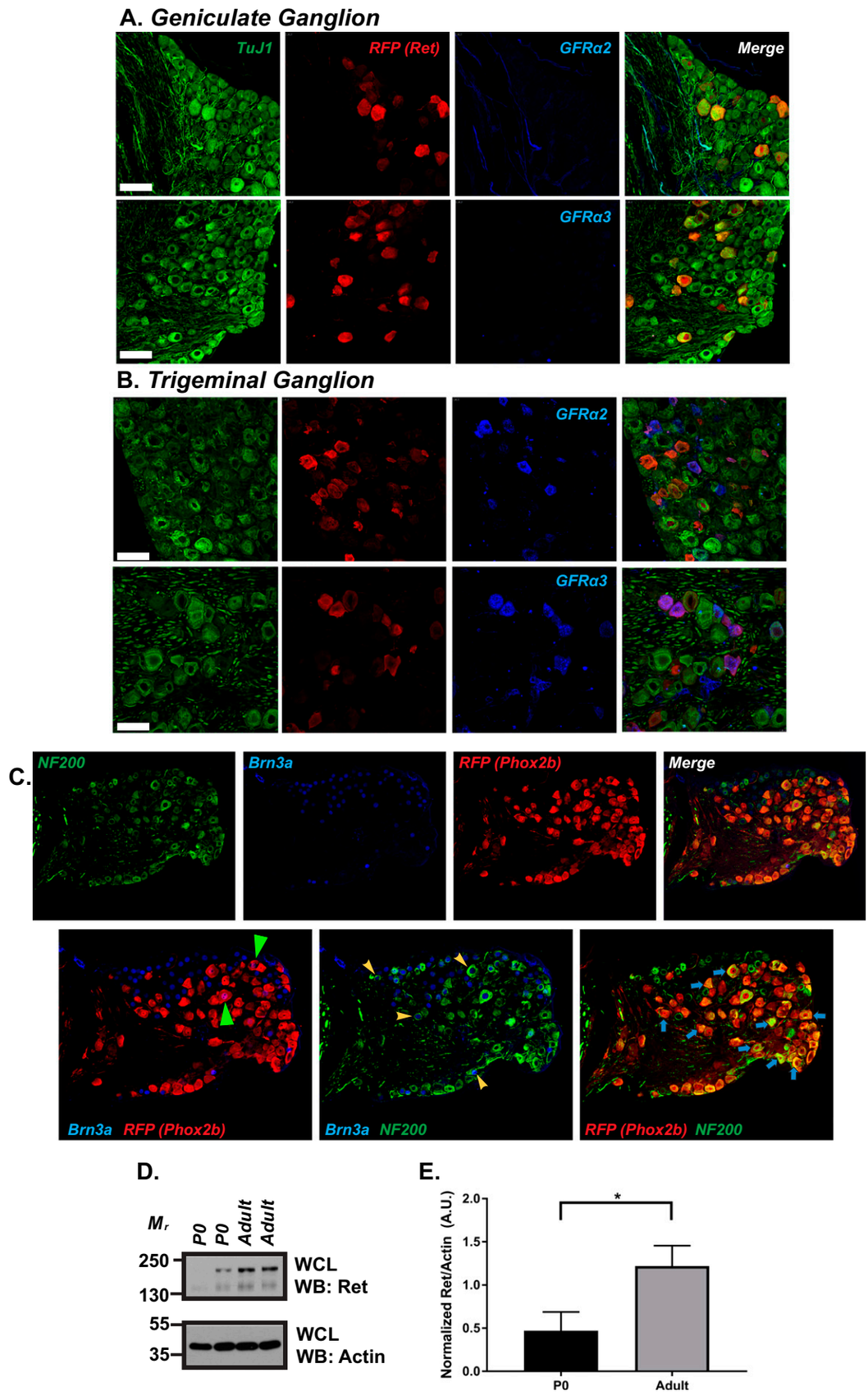

Fig. S6. Expression profile of GFRα2, GFRα3, and NF200 in the geniculate ganglion. (*A*) GGs taken from adult *Ret*-Cre/ER^{T2}; *Rosa26*$^{LSL\text{-}TdTomato/+}$ reporter mice administered TMX were immunostained for TuJ1 (green), RFP (Ret; red), and GFRα2 (blue; *Upper*) or GFRα3 (blue; *Lower*), with the merged images displayed (*Right*). Although some GFRα2+ nerve fibers could be visualized within the nearby facial nerve, no neuronal staining was observed for either coreceptor within the GG. (*B*) To confirm that the GFRα2 and GFRα3 immunostaining procedure was working, we analyzed TGs taken from the mice described above. Clear examples of GFRα2+ (*Upper*) and GFRα3+ (*Lower*) TG neurons were observed, most of which coexpressed Ret. Similar results were obtained in $n = 3$ individual mice with similar results. Collectively, these data indicate that GFRα2 and GFRα3 are not present within GGs, providing further evidence for a GDNF–GFRα1–Ret signaling axis in adult GGs. (*C*) GGs were collected from adult *Rosa26*$^{LSL\text{-}TdTomato/+}$; *Phox2b-Cre*$^{tg/+}$ mice and stained for NF200 (green), Brn3a (blue), and Phox2b (RFP; red) to ascertain the transcriptional profile of NF200+ GG neurons. We observed almost complete segregation of Brn3a and Phox2b expression (*Lower Left* merged), as expected based on previous literature. Rare examples of Brn3a+/Phox2b+ neurons were observed (green arrowheads). While some examples of Brn3a+/NF200+ neurons were observed (*Lower Middle*; yellow arrowheads), many more examples of Phox2b+/NF200+ neurons were observed (*Lower Right*; blue arrows). (*D*) P0 or adult GGs were collected, homogenized, and detergent-extracted, followed by immunoblotting for Ret or actin (as a loading control). (*E*) Quantification of total Ret levels (normalized to actin). We observed a significant increase in adult ($n = 6$) compared with P0 GGs ($n = 5$) ($P = 0.0468$). Error bars indicate mean ± SEM; $^*P < 0.05$. (Scale bars, 50 μm.)

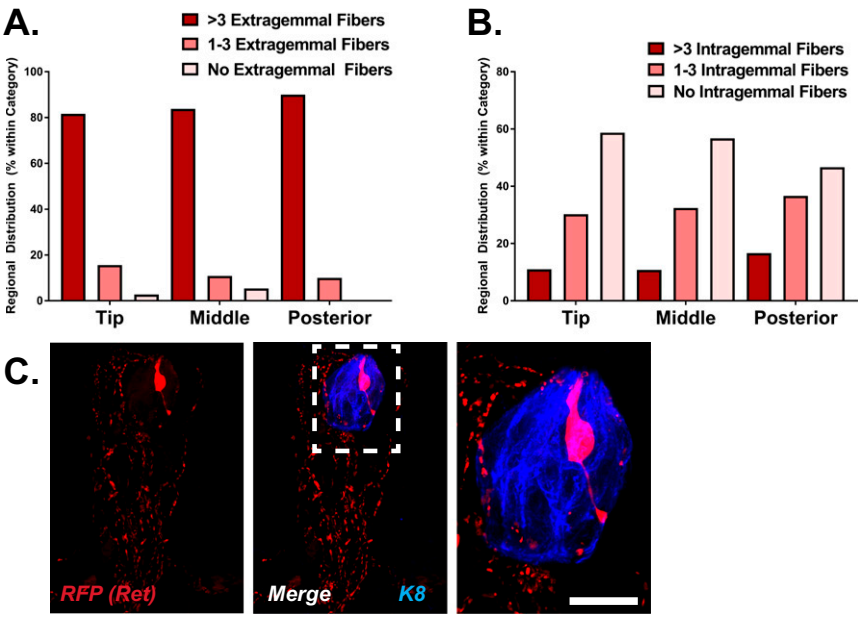

Fig. S7. Characterization of Ret expression in fungiform papillae. (*A*) To determine whether any regional differences in Ret expression existed, we analyzed FPs from adult *Ret*-Cre/ER^{T2}; *Rosa26*$^{LSL\text{-}TdTomato/+}$ reporter tongues labeled with TMX as described in Fig. 5. To control for the increased density of FPs on the tip of the anterior tongue compared with the middle and posterior aspects of the anterior tongue, the number within each group was divided by the total number of FPs within that region to yield a percentage of all FPs counted (n = 5 individual mice). Regardless of regional localization, a similar distribution pattern was observed for extragemmal fibers (>3 fibers/tip: 81.65%; >3 fibers/middle: 83.78%; >3 fibers/posterior: 90.00%; 1 to 3 fibers/tip: 15.59%; 1 to 3 fibers/middle: 10.81%; 1 to 3 fibers/posterior: 10.00%; no fibers/tip: 2.75%; no fibers/middle: 5.41%; no fibers/posterior: 0.00%). (*B*) Similarly, intragemmal fibers were classified to identify potential regional differences as described in *A*. No differences in distribution pattern were observed (>3 fibers/tip: 11.01%; >3 fibers/middle: 10.81%; >3 fibers/posterior 16.67%; 1 to 3 fibers/tip: 30.28%; 1 to 3 fibers/middle: 32.43%; 1 to 3 fibers/posterior: 36.67%; no fibers/tip: 58.72%; no fibers/middle: 56.76%; no fibers/posterior: 46.67%). A small increase overall was seen in intragemmal Ret+ fibers in the posterior region when discounting innervation density categories (53.54% Ret+ intragemmal fibers in posterior vs. 43.24% and 41.29% Ret+ intragemmal fibers in the middle and tip of the anterior tongue, respectively). (*C*) A small number of Ret+ taste receptor cells were observed (8% of FPs overall; always present in the tip of the tongue). These Ret+ TRCs were generally of an elongated morphology, spanning apically to basally within the taste bud. The area within the dashed box in the merged image is magnified (*Right*). (Scale bar, 25 μm.)

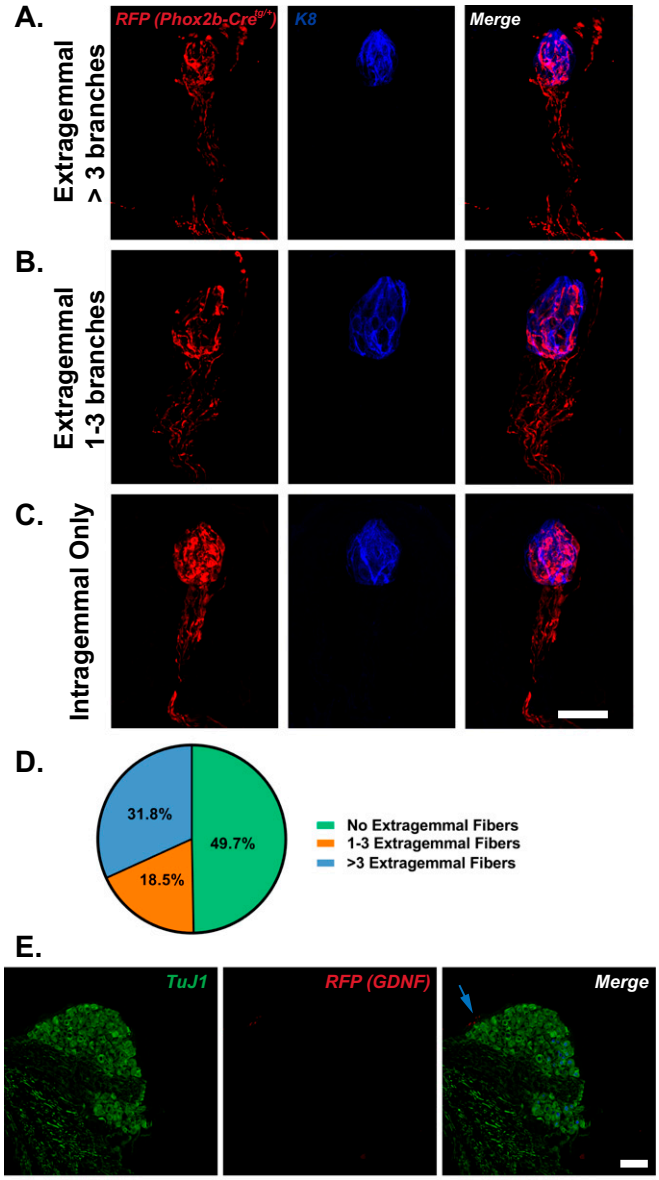

Fig. S8. Many chemosensory nerves terminate outside the taste bud region. (*A*–*C*) To ascertain whether all chemosensory GG neurons projected to the taste bud region proper, tongues were collected from adult *Phox2b*-Cre$^{tg/+}$; *Rosa26*$^{LSL\text{-}TdTomato/+}$ and stained for K8 (blue) and RFP (chemosensory axons; red), with the merged image displayed. One hundred fifty-one fungiform papillae from $n = 5$ individual mice were serially imaged and categorized as having (*A*) >3 extragemmal branches, (*B*) one to three extragemmal branches (≤3), or (*C*) no extragemmal branches (intragemmal only). All FPs analyzed had intragemmal labeling. (Scale bar, 25 μm.) (*D*) A pie chart is used to graphically describe the proportion of FPs within each category. Surprisingly, we observed that 50.3% of FPs had extragemmal labeling in total (31.8% with >3 fibers; 18.5% with one to three fibers), while the remaining 49.7% had no extragemmal labeling. These data may suggest that a substantial portion of FPs have chemosensory axons projecting outside the K8+ region. (*E*) GGs were taken from $n = 4$ adult *GDNF*-IRES-Cre/ER^{T2}; *Rosa26*$^{LSL\text{-}TdTomato/+}$ mice and stained for TuJ1 (green), RFP (indicating GDNF; red), and Phox2b (blue) to ascertain whether GDNF is expressed by GG neurons. No instances of GDNF+ neurons were observed. On occasion, GDNF+ satellite cells within the facial nerve were labeled (blue arrow). (Scale bar, 50 μm.)

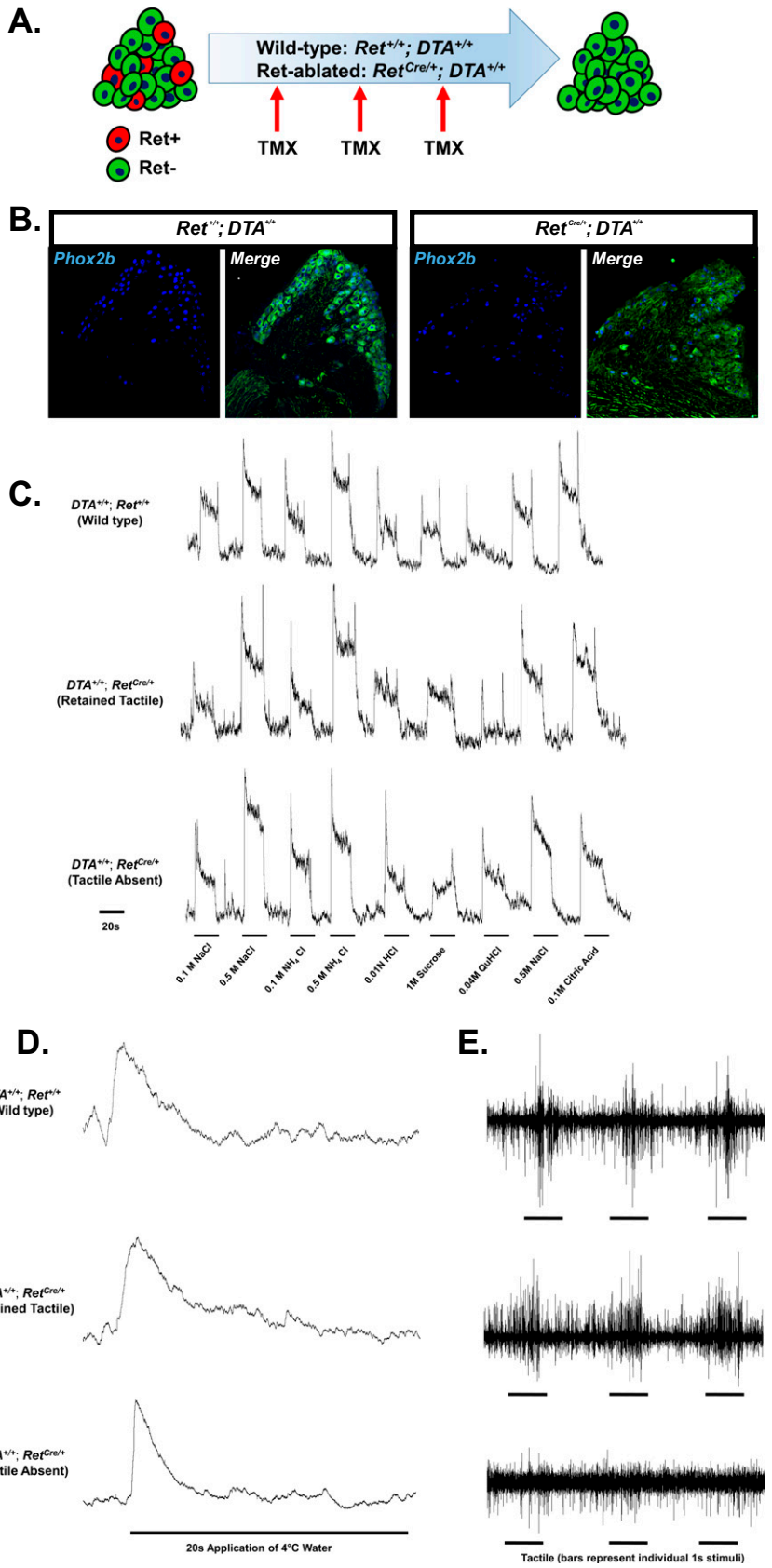

Fig. S9. Additional electrophysiological traces from wild-type and Ret-ablated mice. (*A*) Schematic demonstrating the ablation of Ret+ neurons in vivo before electrophysiological recordings. TMX was administered daily for 3 d, and mice were subsequently utilized for whole-nerve recordings from the chorda tympani. (*B*) GGs from $Ret^{+/+}$; $DTA^{+/+}$ (WT) and $Ret^{Cre/+}$; $DTA^{+/+}$ (Ret-ablated) mice were serially sectioned and immunostained for Phox2b (blue) and TuJ1 (green)

Legend continued on following page

(overlaid in merge). Ret-ablated mice had fewer total numbers of Phox2b+ GG neurons, indicating reliable deletion. (*C*–*E*) Representative chorda tympani integrated nerve responses to various taste stimuli (*C*), 4 °C water (*D*), or raw responses to tactile stimuli (*E*) are displayed. For each panel, the WT animal is displayed in the *Top* trace, while the *Middle* trace represents the electrophysiological responses of a Ret-ablated mouse meeting the inclusion criteria yet retaining tactile responses ($n = 2$). The *Bottom* trace is an additional representative trace from a Ret-ablated mouse with a complete loss of tactile responses ($n = 4$ complete loss; $n = 1$ partial loss).